



## Theoretical Investigation of the Structures and Energetics of (MX)-Ethanol Complexes in the Gas Phase

Ahmed M. SADOON<sup>1\*</sup> 

<sup>1</sup>University of Mosul, College of Education for Pure Science, Department of Chemistry, Mosul, Iraq.

**Abstract:** The structures and energy of alkali halide salt (MX) complexes with ethanol have been investigated in this work. The core of this study is to explore the effect of ion size on the interactions between solvent and solute. LiF and KBr as monovalent salts with different sizes of inion and cation have been chosen to explore this difference in addition to various physical properties. Three complexes of each LiF and KBr with ethanol taking the formula  $\text{MX}(\text{CH}_3\text{CH}_2\text{OH})_n$  ( $n=1-3$ ), were studied. *Ab-initio* calculations have been performed to optimize the chemical structures of these complexes and explore the possible structures, isomers, and their corresponding IR spectra using Density functional theory (DFT/ B3LYP). 6-311G\*\* were chosen as basis sets for these calculations. The geometry evaluations, energy searches, vibrational frequency calculations, and each complex's binding energy were also theoretically extracted in this study. The minimum energy structures were calculated, and different isomers were found. The presence of Ionic hydrogen bonds (IHBs) was observed and proposed to be the main binding between the MX salt and ethanol. Also, the infrared vibrational bands in the OH stretching region were recorded for the minimum structures, and the determined red-shift was at about  $400\text{ cm}^{-1}$ . In addition, the binding energy calculations found a gradual rise in the BE value with every additional ethanol molecule added to MX salt.

**Keywords:** Infrared Spectroscopy, DFT, Alkaline metal, Ethanol.

**Submitted:** July 20, 2022. **Accepted:** November 02, 2022.

**Cite this:** Sadoon AM. Theoretical Investigation of the Structures and Energetics of (MX)-Ethanol Complexes in the Gas Phase. JOTCSA. 2023;10(1):47-54.

**DOI:** <https://doi.org/10.18596/jotcsa.1146250>.

**\*Corresponding author. E-mail:** [ams95@uomosul.edu.iq](mailto:ams95@uomosul.edu.iq)

### 1. INTRODUCTION

The interaction between the salt and solute in polar solutions has been in the spotlight of many studies to understand the behavior of anions and cations in this medium due to their essential role in chemical reactions. In addition to many applications of union and cation behavior in specific fields such as electrochemistry and environmental chemistry (1-3).

The interaction between the salt and polar solvent is usually expressed as *kosmotropic* or *chaotropic*. *Kosmotropic* are called (order-makers), which increase the stability of the hydrogen bonding network, while chaotropic ions (disorder-makers) reduce the stability of the hydrogen bonding grid

and thus reduce the stability of the salt-solvent structures (4, 5).

It is well known that alkaline halides behave as monovalent salts. These salts are dissolved in polar solvents (water, ethanol, etc.) to form separated ions in dilute solutions. The size and charge density of the cation and anion plays a critical role in giving the ability of a single alkaline halide molecule to dissolve in a numerical number of solvent molecules. LiF and KBr were chosen for this study as an example of salt with different sizes and charges of cation and anion.

Lithium fluoride is widely used in industry as an ingredient in lithium-ion battery electrolytes (6). Also, LiF is used as specialized optics for the vacuum ultraviolet spectrum (7) and in light-

emitting diodes production (LED) as a coupling layer to enhance electron injection (8). In addition to many applications in manufacturing nuclear reactors and radiation detectors (9).

Potassium bromide is most commonly used in medical drugs as an anticonvulsant drug to phenobarbital and as an antiepileptic medication for dogs(10), in addition to many other medical and veterinary applications. For industrial applications, KBr plays a significant role in Optics as infrared optical windows and is used widely in components for general spectroscopy (11) and photography as a restrainer by improving differentiation between exposed and unexposed crystals of silver halide to reduce fog(12).

Early studies concentrated on the structure of Alkaline halide (MX) complexes with water (13-16). These studies focused on MX-water complexes geometry structures, infrared (IR), and Mass spectrum using Helium nanodroplet apparatus. The outcome data show the critical role of ionic hydrogen bonds (IHBs) between MX salt and water.

No research has studied the structure of LiF and KBr- ethanol clusters. Only a few studies focused on studying LiF and ethanol's structure separately in the gas phase. LiF as a salt vapor was studied theoretically to investigate the landscape of a numerical number of (LiF)<sub>n</sub> (n=1-8) (17). Ethanol clusters have also been investigated using ab-initio calculations (18), and the thermodynamic properties were recorded in this study.

The theoretical calculation of chemical reactions was widely used in many recent studies, (19-23) due to the unique environment and the ability to study the reactions that cannot be easily prepared in standard lab conditions. The formation of MX-solvent complexes is usually prepared and studied in bulk solutions (19, 20). Even in the diluted solutions, separating MX-(solvent)<sub>n</sub> complexes, where n has a numerical value, is difficult because of the strong ionic hydrogen network (21). Unfortunately, an accurate simulation of the properties is still difficult to record, even in simple electrolytic solutions (22). Considering this limited experimental evidence, the ab-initio calculations study of these complexes looks useful and provides a unique tool to explore the chemistry of these complexes. So, this study will concentrate on studying the interaction of Alkaline halides (MX) with ethanol in gas phase theoretically using ab-initio calculations.

## 2. EXPERIMENTAL

### 2.1. MX(CH<sub>3</sub>OH)<sub>n</sub> formation

LiF and KBr complexes with ethanol (CH<sub>3</sub>OH)<sub>n</sub>, (n=1-3) were shaped using the Chemcraft software package (23). The premier structures were created with different positions and randomly rotated for MX and ethanol molecules to examine a wide range of potential geometries and isomers of MX(CH<sub>3</sub>OH)<sub>n</sub> complexes. The structure geometries were then optimized to find the minimum structures of each complex using ab-initio calculations.

#### 2.1.1. Ab-initio calculations

Ab-initio calculations were applied using Density functional theory (DFT) with Becke three-parameter exchange and Lee-Yang-Parr correlation (B3LYP) within the Gaussian 03 software package (24). The basis set (6-311G\*\*) obtained from the EMSL basis set exchange library (25) was then used to optimize the formatted structures. Each complex's minimum energy isomer structure was used to extract the data of geometry, energy, and infrared (IR) spectra (vibrational frequency values). In order to reduce the calculation time, the Hartree-Fock (HF) level of theory was first used with (6-311G\*\*) bases set to evaluate the optimized structures. The optimized structures at the HF level were then re-optimized using the DFT(b3lyp) level of theory at the same basis set. A scaling factor of 0.967 was used to correct the values of vibrational frequencies of the final optimized structures. This factor is advised by the National Institute of Standards and Technology (NIST) for the DFT/B3LYP level of theory (26).

#### 2.1.2. Geometry and structure

The final optimized structures of each complex were utilized to extract the information on the minimum energy of isomers, frequencies in the region of OH stretching bands, bond length, angles, dihedral angle, and the Binding Energy (BE). These results were obtained using Chemcraft software.

## 3. RESULTS AND DISCUSSION

### 3.1. MX(CH<sub>3</sub>CH<sub>2</sub>OH)<sub>n</sub> structures

#### 3.1.1. LiF(CH<sub>3</sub>CH<sub>2</sub>OH)<sub>n</sub> structures

Several isomers were applied in DFT calculations for LiF(CH<sub>3</sub>CH<sub>2</sub>OH)<sub>n</sub> complexes. For LiF(CH<sub>3</sub>CH<sub>2</sub>OH) complex, two optimized structures were found for this complex among many tested isomers, see Figure 1. The global minimum structure shows that the LiF salt takes the position so that the hydrogen ion of the hydroxyl group can form IHB with the fluoride atom. The higher energy structure shows that the methyl group in ethanol forms an IHB with a fluoride atom. The length of IHB in the minimum structure is about 1.68 Å while 2.203 Å in the higher energy isomer. Additional stabilization comes from the Li<sup>+</sup> ion to the O<sup>-</sup> atom.

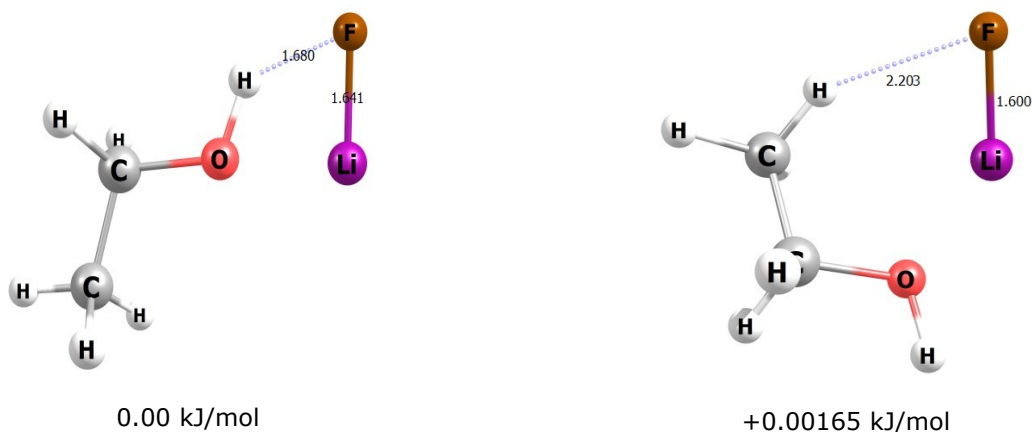


**Figure 1:** The minima structures for  $\text{LiF}(\text{CH}_3\text{CH}_2\text{OH})$  with their energies in kJ/mol using DFT/B3LYP level of theory and 6-311G\*\* as basis set

Three minima structures were recorded for  $\text{LiF}(\text{CH}_3\text{CH}_2\text{OH})_2$ , as can be seen in Figure 2. The global minimum structure is similar to the  $n = 1$  complex but now has two IHBs bonding the fluoride ion and the H atoms of the hydroxyl group. The following minimum structure has an energy of 23.31 kJ/mol, higher than the global minimum structure energy, and also has two IHBs between the hydrogen of each ethanol methyl group and fluoride ion. The bond length of these two structures were 1.744 and 1.654 Å, respectively. The last structure

had energy above the global minimum structure at about 38.33 kJ/mol. Two ethanol molecules of this structure interacted with each other via one IHB. Another IHB seen in this structure bonded the hydrogen atom of the ethanol methyl group with the fluoride ion. The significant point seen in this complex, compared with  $\text{LiF}(\text{CH}_3\text{CH}_2\text{OH})$  complex, is the difference in LiF bond length in the minimum structures that increased from 1.641 Å to 1.744 Å. This difference may be related to the reduction of fluoride ion charge bonded to a couple of IHBs.

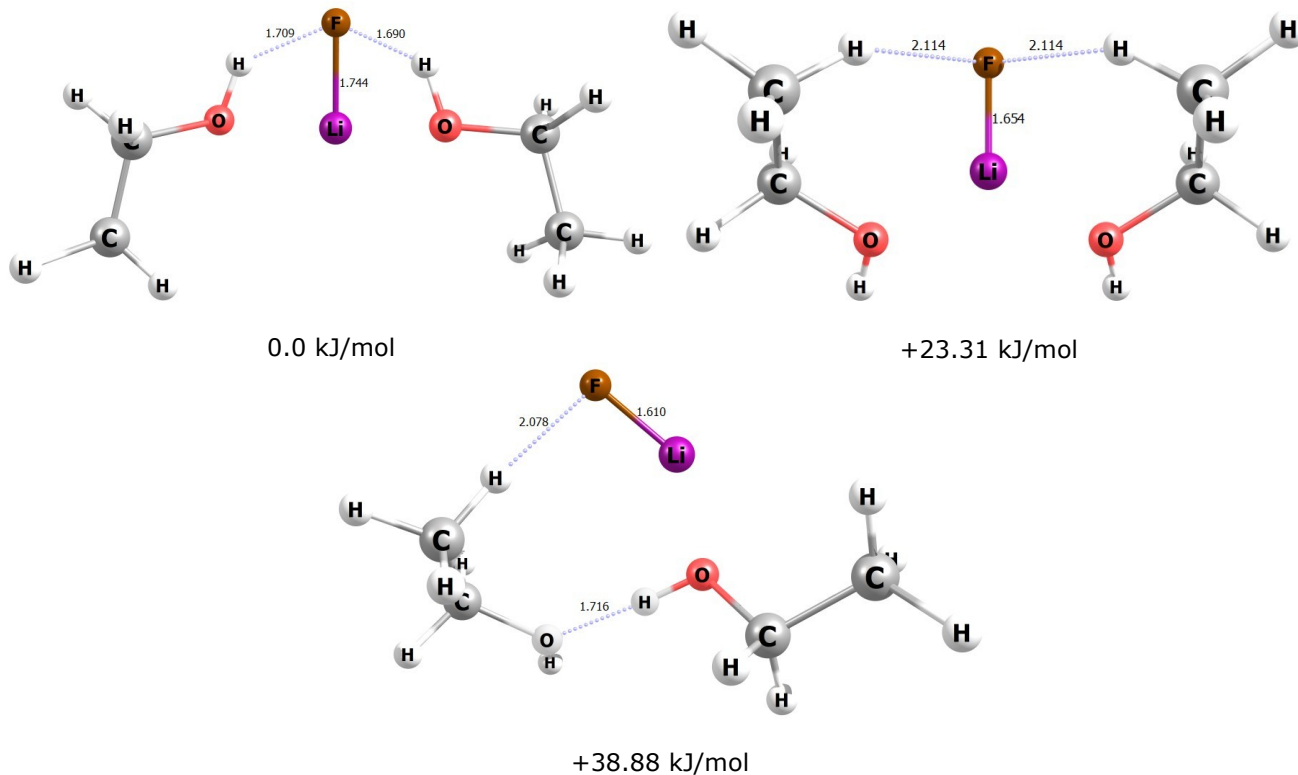


**Figure 2:** The minima structures for  $\text{LiF}(\text{CH}_3\text{CH}_2\text{OH})_2$  with their energies in kJ/mol using DFT/B3LYP level of theory and 6-311G\*\* as basis set

For  $n = 3$ , Three minima structures were found; see Figure 3. The global minimum for  $\text{LiF}(\text{CH}_3\text{CH}_2\text{OH})_3$  is similar to those found for  $\text{LiF}(\text{CH}_3\text{CH}_2\text{OH})$  and  $\text{LiF}(\text{CH}_3\text{CH}_2\text{OH})_2$ . Three ethanol molecules were bonded to fluoride ion by 3 IHBs between the F atom and the hydrogen of the hydroxyl group. The other isomer has higher energy from the global

minimum structure of about 9.74 kJ/mol. This isomer takes the formula where three ethanol bonded together via two IHBs and with one IHB with fluoride ion. The last isomer bonded to LiF salt via three IHBs similar to  $\text{LiF}(\text{CH}_3\text{CH}_2\text{OH})_2$ . LiF bonds in the three structures were about 1.91, 1.644, and 1.695 Å, respectively.

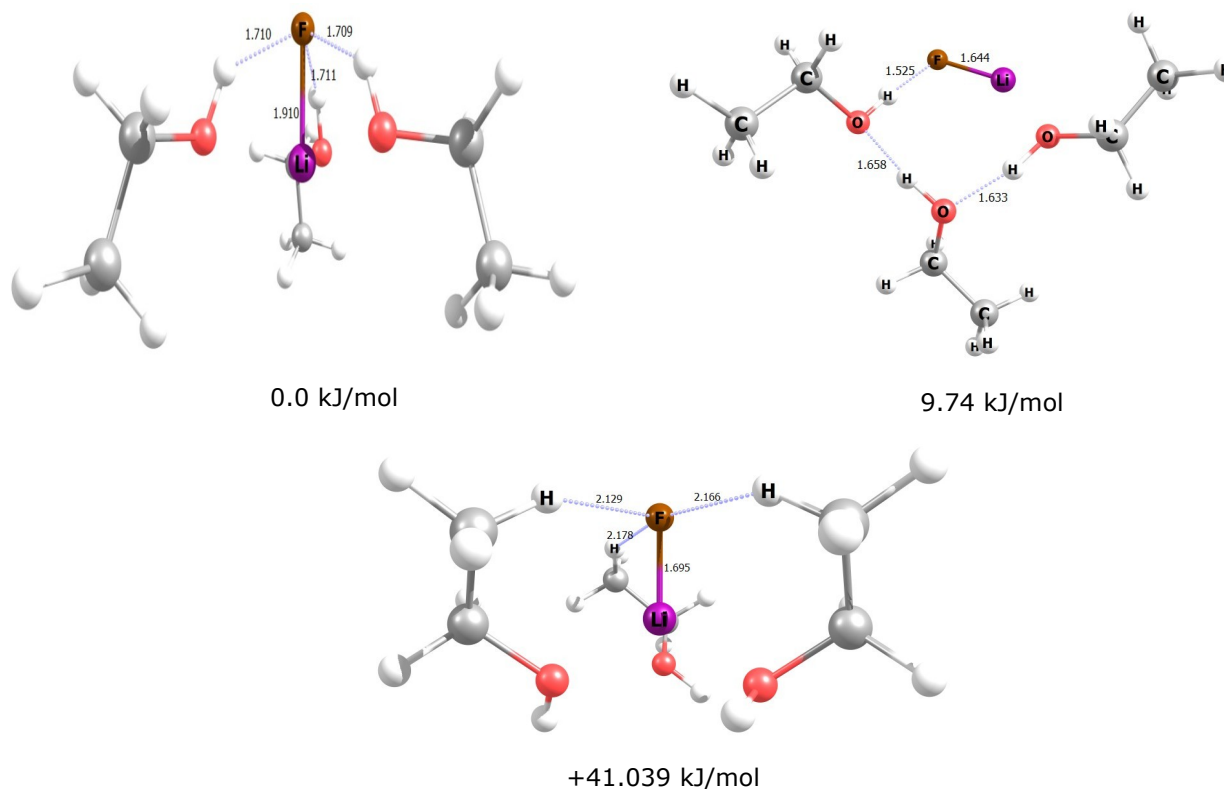


**Figure 3:** The minima structures for  $\text{LiF}(\text{CH}_3\text{CH}_2\text{OH})_3$  with their energies in kJ/mol using DFT/B3LYP level of theory and 6-311G\*\* as basis set.

### 3.1.2. $\text{KBr}(\text{CH}_3\text{CH}_2\text{OH})_n$ structures

The *ab-initio* calculations for  $\text{KBr}(\text{CH}_3\text{CH}_2\text{OH})_n$  ( $n=1-3$ ) were found and seen in Figures 4, 5, and 6, respectively. No significant changes were observed in these structures for these complexes compared with  $\text{LiF}(\text{CH}_3\text{CH}_2\text{OH})_n$  calculations. A significant difference in  $\text{KBr}(\text{CH}_3\text{CH}_2\text{OH})_n$  complexes was seen

in the IHBs, which were longer than the IHBs in the  $\text{LiF}(\text{CH}_3\text{CH}_2\text{OH})_n$  structures, due to the low electronegativity of Br atom compared with Li atom electronegativity. For KBr bond length, it increased gradually with every additional ethanol molecule and gave 2.95, 3.09, and 3.29 Å, respectively, for the  $\text{KBr}(\text{CH}_3\text{CH}_2\text{OH})_n$  ( $n=1-3$ ) minimum structures.

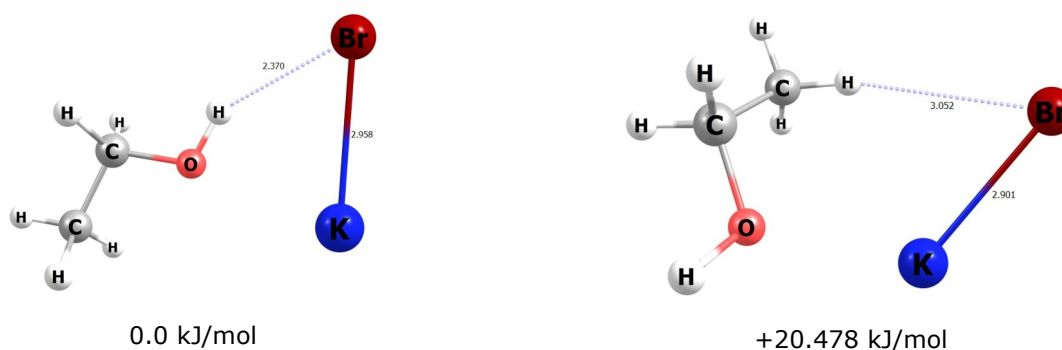


**Figure 4:** The calculated structures for  $\text{MgCl}_2(\text{H}_2\text{O})$  with their energies in kJ/mol using DFT/B3LYP level of theory and 6-311G\*\* as basis set.

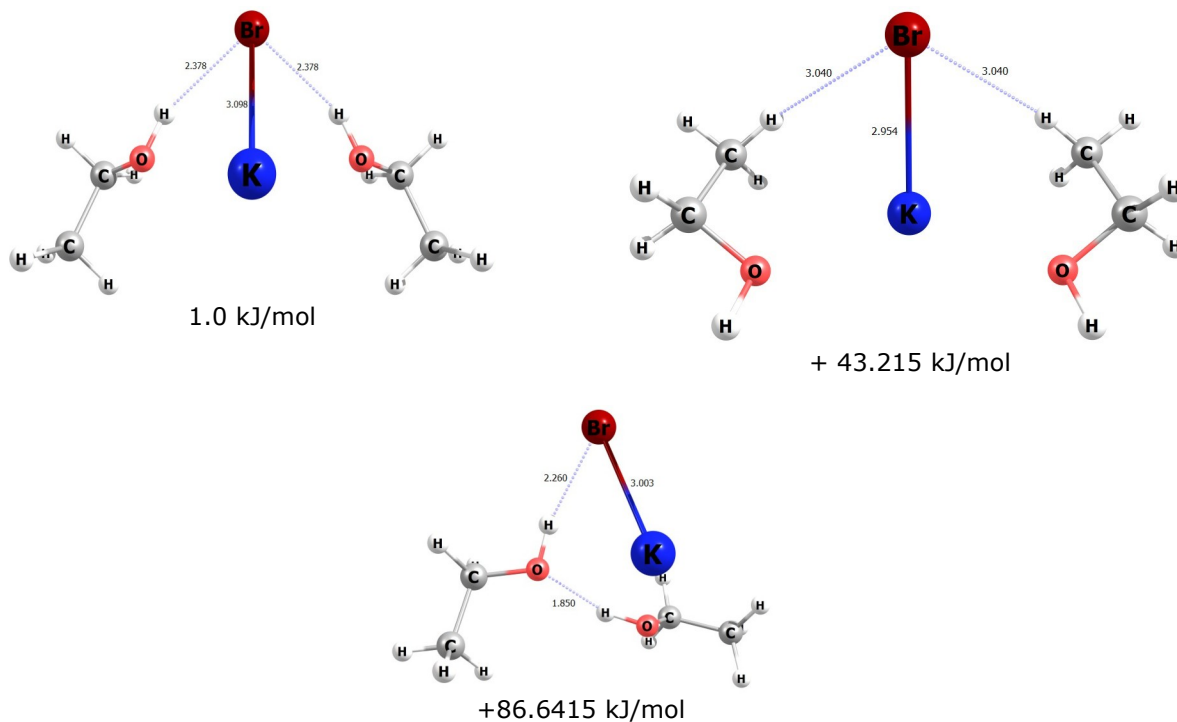


**Figure 5:** The calculated structures for  $MgCl_2(H_2O)_2$  with their energies in kJ/mol using DFT/B3LYP level of theory and 6-311G\*\* as basis set.

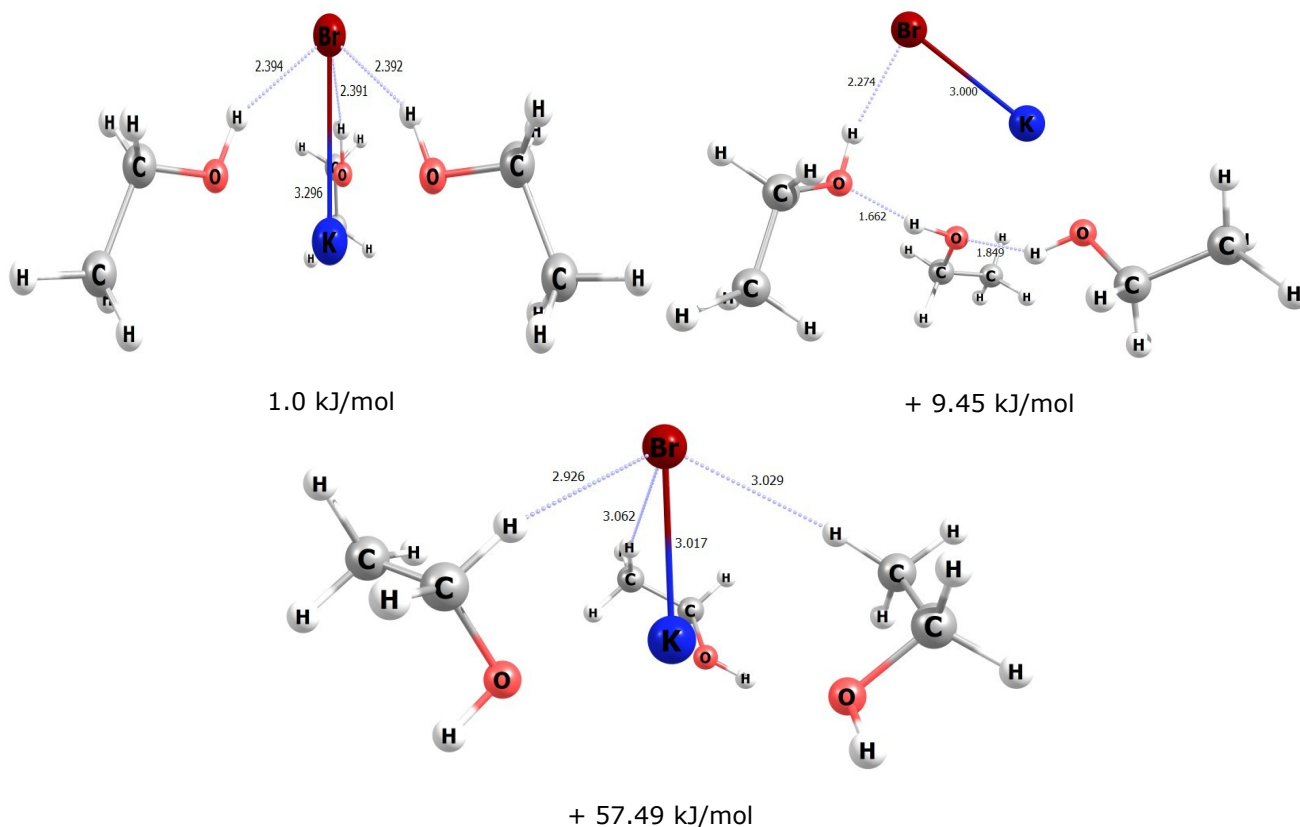


**Figure 6:** The calculated structures for  $MgCl_2(H_2O)_3$  with their energies in kJ/mol using DFT/B3LYP level of theory and 6-311G\*\* as basis set.

### 3.2. Infrared Spectra of $\text{MX}(\text{CH}_3\text{CH}_2\text{OH})_n$ Complexes

Infrared spectra of  $\text{LiF}(\text{CH}_3\text{CH}_2\text{OH})_n$ ,  $n=1-3$ , were assigned theoretically using the DFT/B3LYP level of theory on the OH stretching region to evaluate the effect of IHBs on the OH symmetric stretching band. The stretching frequency values were corrected using a scaling factor of 0.967. Only global minimum structures were chosen for IR analysis.

The prediction of DFT calculations at the OH symmetric stretching frequencies is summarized in Table 1. In general, the absorption of OH bands of  $\text{LiF}(\text{CH}_3\text{CH}_2\text{OH})_n$  complexes are red-shifted from the OH stretching band of the free ethanol molecule that is seen at  $3721\text{ cm}^{-1}$ . This trend of OH stretching red-shift has been recorded previously in several studies(13, 27, 28). The OH band frequency of the  $\text{LiF}(\text{CH}_3\text{CH}_2\text{OH})$  complex was found in  $3149\text{ cm}^{-1}$  and then raised to  $3208\text{ cm}^{-1}$  for  $\text{LiF}(\text{CH}_3\text{CH}_2\text{OH})_2$  and  $3263\text{ cm}^{-1}$  for  $\text{LiF}(\text{CH}_3\text{CH}_2\text{OH})_3$ . This red shift can be attributed to the OH band,

which bonded to the fluoride ion via an ionic hydrogen bond (IHB). This behavior of OH frequency fluctuation can be assigned to the high electronegativity of the Fluoride atom in the  $n=1$  complex. This electronegativity has decreased gradually with every additional ethanol molecule. Therefore, OH frequency has increased again in  $n=2$  and 3 complexes.

The same trend of OH stretching frequency behavior in  $\text{LiF}(\text{CH}_3\text{CH}_2\text{OH})_n$  complexes was seen for the minimum structures of  $\text{KBr}(\text{CH}_3\text{CH}_2\text{OH})_n$ ,  $n=1-3$ , complexes. Red shifts of OH stretching bands were recorded in these complexes due to IHBs effect on bromide electronegativity reduced more with every additional ethanol molecule. The *ab-initio* calculations recorded the OH symmetric stretching frequency of  $\text{KBr}(\text{CH}_3\text{CH}_2\text{OH})$  at  $3318\text{ cm}^{-1}$ . For  $\text{KBr}(\text{CH}_3\text{CH}_2\text{OH})_n$  where  $n=2$  and 3, the OH symmetric stretching band was observed at  $3346\text{ cm}^{-1}$  and  $3382\text{ cm}^{-1}$ , respectively; see Table 2.

**Table 1:** Infrared spectra for the minimum structures of  $\text{LiF}(\text{CH}_3\text{CH}_2\text{OH})_n$  ( $n=1-3$ ) complexes for the OH stretching region using DFT/B3LYP level of theory.

OH frequency band/ $\text{cm}^{-1}$	Vibration frequency assignment	Complex
<b>3149</b>	symmetric stretching	$\text{LiF}(\text{CH}_3\text{CH}_2\text{OH})$
<b>3208</b>	symmetric stretching	$\text{LiF}(\text{CH}_3\text{CH}_2\text{OH})_2$
3266	asymmetric stretching	
<b>3263</b>	symmetric stretching	$\text{LiF}(\text{CH}_3\text{CH}_2\text{OH})_3$
3265	asymmetric stretching	
3336	asymmetric stretching	

**Table 2:** Infrared spectra for the minimum structures of  $\text{KBr}(\text{CH}_3\text{CH}_2\text{OH})_n$  ( $n=1-3$ ) complexes for the OH stretching region using DFT/B3LYP level of theory.

OH frequency band/ $\text{cm}^{-1}$	Vibration frequency assignment	Complex
<b>3318</b>	symmetric stretching	$\text{KBr}(\text{CH}_3\text{CH}_2\text{OH})$
<b>3346</b>	symmetric stretching	$\text{KBr}(\text{CH}_3\text{CH}_2\text{OH})_2$
3370	asymmetric stretching	
<b>3382</b>	symmetric stretching	$\text{KBr}(\text{CH}_3\text{CH}_2\text{OH})_3$
3384	asymmetric stretching	
3414	asymmetric stretching	

### 3.3. Binding energy calculations for $\text{MX}(\text{CH}_3\text{CH}_2\text{OH})_n$ ( $n = 1-3$ ) complexes

The Binding energy (BE) of the global minimum structure of  $\text{MX}(\text{CH}_3\text{CH}_2\text{OH})_n$  complexes was calculated from the DFT/B3LYP calculations and summarized in Table 3 for  $\text{LiF}(\text{CH}_3\text{CH}_2\text{OH})_n$  and in Table 4 for  $\text{KBr}(\text{CH}_3\text{CH}_2\text{OH})_n$  complexes. The BE was calculated using the following equation:

$$\text{BE} = \Delta E = E(\text{MX}(\text{CH}_3\text{CH}_2\text{OH})_n) - (E(\text{MX}) + E(\text{CH}_3\text{CH}_2\text{OH})_n)$$

In general, a gradual increase in the values of BE was seen in both  $\text{MX}(\text{CH}_3\text{CH}_2\text{OH})_n$  complexes, where ( $n=1-3$ ), with increasing  $n$  value of ethanol. Also, the BE of  $\text{LiF}(\text{CH}_3\text{CH}_2\text{OH})_n$  complexes were higher than the BE of  $\text{KBr}(\text{CH}_3\text{CH}_2\text{OH})_3$  complexes. This difference may relate to the high

electronegativity of F<sup>-</sup> ion in contrast with Br<sup>-</sup> ion electronegativity. The BE of LiF(CH<sub>3</sub>CH<sub>2</sub>OH)<sub>n</sub> and KBr(CH<sub>3</sub>CH<sub>2</sub>OH)<sub>n</sub> complexes can be seen in Tables 3 and 4, respectively.

The BE of the minimum structures of LiF(CH<sub>3</sub>CH<sub>2</sub>OH)<sub>n</sub>, n=1-3, were (102, 197, and 282)

kJ/mol respectively. On the other hand, The BE of the minimum structure of KBr(CH<sub>3</sub>CH<sub>2</sub>OH)<sub>n</sub>, n=1-3, complexes were (75, 146, and 212) kJ/mol, respectively. This increase may come from the additional IHBs and the proximity of M<sup>+</sup> ion to O atom of the hydroxyl group that increased with every additional ethanol molecule.

**Table 3:** The binding energy of LiF(CH<sub>3</sub>CH<sub>2</sub>OH)<sub>n</sub> (n = 1–3) complexes using DFT/B3LYP level of theory.

Binding Energy kJ/mol	Complex
102.37	LiF(CH <sub>3</sub> CH <sub>2</sub> OH)
197.90	LiF(CH <sub>3</sub> CH <sub>2</sub> OH) <sub>2</sub>
282.24	LiF(CH <sub>3</sub> CH <sub>2</sub> OH) <sub>3</sub>

**Table 4:** The binding energy of KBr(CH<sub>3</sub>CH<sub>2</sub>OH)<sub>n</sub> (n = 1–3) complexes using DFT/B3LYP level of theory.

Binding Energy kJ/mol	Complex
75.04	KBr(CH <sub>3</sub> CH <sub>2</sub> OH)
146.23	KBr(CH <sub>3</sub> CH <sub>2</sub> OH) <sub>2</sub>
212.82	KBr(CH <sub>3</sub> CH <sub>2</sub> OH) <sub>3</sub>

#### 4. CONCLUSION

Structure parameters, Infrared spectra (IR), and the Binding Energy of MX(CH<sub>3</sub>CH<sub>2</sub>OH)<sub>n</sub> complexes, where n = 1–3 and MX =LiF and KBr, have been performed in this work using *Ab-initio* calculations. Several isomers of these complexes have been recorded. A significant observation was seen for MX(CH<sub>3</sub>CH<sub>2</sub>OH)<sub>n</sub> complexes that show a significant increase in the M-X bond length. This increment comes from the effect of the ethanol hydroxyl group that inserts between M and X ions and reduces their interaction by forming IHBs. The global minimum structures of complexes were then used to extract the information on the Vibrational frequency bands in OH stretching regions and the binding energy. The formation of IHBs was observed between the hydrogen of the ethanol hydroxyl group. For IR spectra, a Red-shift in the positions of the OH stretching bands was seen, which is consistent with the presence of the IHBs. Also, a significant increase in the Binding energy (BE) was seen with the increasing n value of ethanol. This increase indicated that the IHB and the proximity of the M<sup>+</sup> ion to the O atom play a critical role in MX(CH<sub>3</sub>CH<sub>2</sub>OH)<sub>n</sub> complexes.

#### 5. ACKNOWLEDGMENTS

The author is grateful to the University of Mosul and the Chemistry department at the College of Education for pure sciences for their support and funding of this work.

#### 6. REFERENCES

- Satchell DPN. Ions in solution: Basic principles of chemical interactions. Endeavour [Internet]. 1988 Jan [cited 2022 Nov 27];12(4):195. Available from: [<URL>](#)
- Marcus Y. Ions in Solution and their Solvation: Marcus/Ions in Solution and their Solvation [Internet]. Hoboken, NJ: John Wiley & Sons, Inc; 2015 [cited 2022 Nov 27]. Available from: [<URL>](#)
- Friedman HaroldL. Ionic hydration in chemistry and biophysics. Journal of Electroanalytical Chemistry and Interfacial Electrochemistry [Internet]. 1982 Jan [cited 2022 Nov 27];131:407–8. Available from: [<URL>](#)
- Marcus Y. Effect of ions on the structure of water. Pure and Applied Chemistry [Internet]. 2010 Jun 19 [cited 2022 Nov 27];82(10):1889–99. Available from: [<URL>](#)
- Moelbert S, Normand B, De Los Rios P. Kosmotropes and chaotropes: modelling preferential exclusion, binding and aggregate stability. Biophysical Chemistry [Internet]. 2004 Dec [cited 2022 Nov 27];112(1):45–57. Available from: [<URL>](#)
- Aigueperse J, Mollard P, Devilliers D, Chemla M, Faron R, Romano R, et al. Fluorine Compounds, Inorganic. In: Wiley-VCH Verlag GmbH & Co. KGaA, editor. Ullmann's Encyclopedia of Industrial Chemistry [Internet]. Weinheim, Germany: Wiley-VCH Verlag GmbH & Co. KGaA; 2000 [cited 2022 Nov 27]. p. a11\_307. Available from: [<URL>](#)
- Zheng Y, Song W, Mo W ting, Zhou L, Liu JW. Lithium fluoride recovery from cathode material of spent lithium-ion battery. RSC Adv [Internet]. 2018 [cited 2022 Nov 27];8(16):8990–8. Available from: [<URL>](#)



8. Andeen C, Fontanella J, Schuele D. Low-Frequency Dielectric Constant of LiF, NaF, NaCl, NaBr, KCl, and KBr by the Method of Substitution. *Phys Rev B* [Internet]. 1970 Dec 15 [cited 2022 Nov 27];2(12):5068–73. Available from: [<URL>](#)
9. McGregor DS, Bellinger SL, Shultis JK. Present status of microstructured semiconductor neutron detectors. *Journal of Crystal Growth* [Internet]. 2013 Sep [cited 2022 Nov 27];379:99–110. Available from: [<URL>](#)
10. De Lahunta A, Glass E, Kent M. *Veterinary Neuroanatomy and Clinical Neurology* [Internet]. Elsevier; 2009 [cited 2022 Nov 27]. Available from: [<URL>](#)
11. Alpert NL, Keiser WE., Szymanski HA. *IR: Theory and Practice of Infrared Spectroscopy*. Cham: Springer International Publishing; 2012. 381 p.
12. Anchell S. *The Film Developing Cookbook* [Internet]. 1st ed. Routledge; 1998 [cited 2022 Nov 27]. Available from: [<URL>](#)
13. Tandy J, Feng C, Boatwright A, Sarma G, Sadoon AM, Shirley A, et al. Communication: Infrared spectroscopy of salt-water complexes. *The Journal of Chemical Physics* [Internet]. 2016 Mar 28 [cited 2022 Nov 27];144(12):121103. Available from: [<URL>](#)
14. Sadoon AM, Sarma G, Cunningham EM, Tandy J, Hanson-Heine MWD, Besley NA, et al. Infrared Spectroscopy of NaCl(CH<sub>3</sub>OH)<sub>n</sub> Complexes in Helium Nanodroplets. *J Phys Chem A* [Internet]. 2016 Oct 20 [cited 2022 Nov 27];120(41):8085–92. Available from: [<URL>](#)
15. Li RZ, Liu CW, Gao YQ, Jiang H, Xu HG, Zheng WJ. Microsolvation of LiI and CsI in Water: Anion Photoelectron Spectroscopy and ab initio Calculations. *J Am Chem Soc* [Internet]. 2013 Apr 3 [cited 2022 Nov 27];135(13):5190–9. Available from: [<URL>](#)
16. Mizoguchi A, Ohshima Y, Endo Y. The study for the incipient solvation process of NaCl in water: The observation of the NaCl-(H<sub>2</sub>O)<sub>n</sub> (n = 1, 2, and 3) complexes using Fourier-transform microwave spectroscopy. *The Journal of Chemical Physics* [Internet]. 2011 Aug 14 [cited 2022 Nov 27];135(6):064307. Available from: [<URL>](#)
17. Doll K, Schön JC, Jansen M. Ab initio energy landscape of LiF clusters. *The Journal of Chemical Physics* [Internet]. 2010 Jul 14 [cited 2022 Nov 27];133(2):024107. Available from: [<URL>](#)
18. Umer M, Kopp WA, Leonhard K. Efficient yet accurate approximations for ab initio calculations of alcohol cluster thermochemistry. *The Journal of Chemical Physics* [Internet]. 2015 Dec 7 [cited 2022 Nov 27];143(21):214306. Available from: [<URL>](#)
19. Sangoro J, Cosby T, Kremer F. Rotational and Translational Diffusion in Ionic Liquids. In: Paluch M, editor. *Dielectric Properties of Ionic Liquids* [Internet]. Cham: Springer International Publishing; 2016 [cited 2022 Nov 27]. p. 29–51. (Advances in Dielectrics). Available from: [<URL>](#)
20. Nancollas GH. The thermodynamics of metal-complex and ion-pair formation. *Coordination Chemistry Reviews* [Internet]. 1970 Dec [cited 2022 Nov 27];5(4):379–415. Available from: [<URL>](#)
21. Meot-Ner (Mautner) M. Update 1 of: Strong Ionic Hydrogen Bonds. *Chem Rev* [Internet]. 2012 Oct 10 [cited 2022 Nov 27];112(10):PR22–103. Available from: [<URL>](#)
22. Eisenberg B. Ionic Interactions Are Everywhere. *Physiology* [Internet]. 2013 Jan [cited 2022 Nov 27];28(1):28–38. Available from: [<URL>](#)
23. Zhurko G, Zhurko D. Chemcraft-graphical software for visualization of quantum chemistry computations [Internet]. 2016. Available from: [<URL>](#)
24. Frisch MJ, Trucks GW, Schlegel HB, Scuseria GE, Robb MA, Cheeseman JR, et al. *Gaussian 03, Revision C.02* [Internet]. Gaussian, Inc.; 2004. Available from: [<URL>](#)
25. Schuchardt KL, Didier BT, Elsethagen T, Sun L, Gurumoorhi V, Chase J, et al. Basis Set Exchange: A Community Database for Computational Sciences. *J Chem Inf Model* [Internet]. 2007 May 1 [cited 2022 Nov 27];47(3):1045–52. Available from: [<URL>](#)
26. Johnson R. Computational Chemistry Comparison and Benchmark Database, NIST Standard Reference Database 101 [Internet]. National Institute of Standards and Technology; 2002 [cited 2022 Nov 27]. Available from: [<URL>](#)
27. Cabarcos OM, Weinheimer CJ, Martínez TJ, Lisy JM. The solvation of chloride by methanol—surface versus interior cluster ion states. *The Journal of Chemical Physics* [Internet]. 1999 May 15 [cited 2022 Nov 27];110(19):9516–26. Available from: [<URL>](#)
28. Beck JP, Lisy JM. Cooperatively Enhanced Ionic Hydrogen Bonds in Cl – (CH<sub>3</sub>OH)<sub>1–3</sub> Ar Clusters. *J Phys Chem A* [Internet]. 2010 Sep 23 [cited 2022 Nov 27];114(37):10011–5. Available from: [<URL>](#)